



Adsorption of Zn(II) ions from aqueous solution on lignite-fired fly ash

T.S. Malarvizhi, T. Santhi*

*Department of Chemistry, Karpagam University, Coimbatore 641021, India
Email: info@karpagam.com*

Received 19 April 2012; Accepted 30 January 2013

ABSTRACT

Batch experiments were carried out under various adsorbent dosages, pH, contact time, and different metal ion concentrations. For fly ash before washing (BFA), under the optimum conditions of flyash dosages of 4 g L^{-1} at pH 7, temperature at 303 K and contact time of 1 h, the removal of the Zn(II) was 8.3%. But for Fly ash after washing(AFA), under the optimum conditions of fly ash dosages of 4 g L^{-1} at pH equal to 4, temperature at 303 K and contact time of 1 h, the removal of the Zn(II) was 57.3%. For both adsorbents, the adsorption of Zn (II) ions onto fly ash followed the pseudo-second-order kinetics. The Langmuir isotherm model well fitted to BFA and AFA adsorbents for the adsorption of Zn(II) ions compared with other isotherm models shows the monolayer homogeneous adsorption on both the adsorbents. A high percentage of removal of Zn(II) ion observed at pH 4 for the adsorbent AFA. The maximum removal of about 91.43% of Zn(II) ions was obtained at pH 4.0 for adsorbent dose of $1\text{ g}/50\text{ mL}$ of 100 ppm metal ion compared with BFA which was only 20.77% at the pH 7.

Keywords: Fly ash; Zn(II) ions adsorption; Kinetics; Isotherms

1. Introduction

The pollution of water resources due to the indiscriminate disposal of heavy metals has been causing worldwide concern for the last decades. It is well known that some metals can have toxic or harmful effects on many forms of life. Among the most toxic metals, Cr, Cu, Pb, Zn, and Hg which is one of the 11 hazardous priority substances in the list of pollutants contained in the water framework directive (Directive 2000/60/EC) [1]. Heavy metals are resulting from industries [2] (electroplating, fertilizers, pesticides, and pigments manufacturing) in huge amounts of wastewater with compositions ranging from tenth up

to thousands of mg L^{-1} . For avoiding flora, fauna, and health problems, the discharge limits are strict and require advanced wastewater treatment process.

Various treatment technologies have been developed for the purification of water and wastewater contaminated by heavy metals. The common methods used for the removal of metal ions from industrial effluents include: chemical precipitation, solvent extraction, reverse osmosis, ultra filtration, ion exchange, and adsorption. Among these methods, adsorption has been an effective separation process for a wide variety of applications. Since activated carbon is expensive, an alternate inexpensive adsorbent that drastically reduces the cost of adsorption system has always been searched [3,4].

*Corresponding author.

For fulfilling the industrial requirements, low-cost adsorbents are intensively studied mainly based on natural compounds or on wastes. Heavy metals removal was reported on inorganic oxides [5]. Previous studies investigated FA as substrate for heavy metals (Cd, Co, Zn, & Ni) removal resulted from industries. FA is porous solid product produced from combustion of coal (or) Lignite in thermoelectric power plants. It consists of SiO_2 , Al_2O_3 , CaO , and Fe_2O_3 as its major constituents with varying amounts of unburnt carbon. Part of the ash is being used in cement and bricks manufacturing, but large amount are still free and represent major pollutant source. Most of the FA is dumped without any necessary pre-treatment. Thus, making a productive reuse of FA is practically urgent and it may bring considerable environmental benefits. One possible alternative is to develop an alternative process (like wastewater treatment) involving the use of this waste [6].

This paper presents a study developed on fly ash before and after washing (BFA and AFA) using different kinetic equations and different isotherms. The objective of this paper is to study the effect of various parameters on the extent of removal of Zn(II) ions, to optimize the parameters and apply various adsorption isotherms and kinetic equations to the adsorption data.

2. Materials and methods

The fly ash used for this study was collected from the NLC Power Plant, Neyveli, Tamil Nadu, India. Part of the fly ash was washed with double distilled water for 24 h with stirring. It was then filtered and dried in hot air oven at a temperature of 105°C . The dried fly ash (AFA) was then used for further studies [7]. The other part of the fly ash was used without washing (BFA).

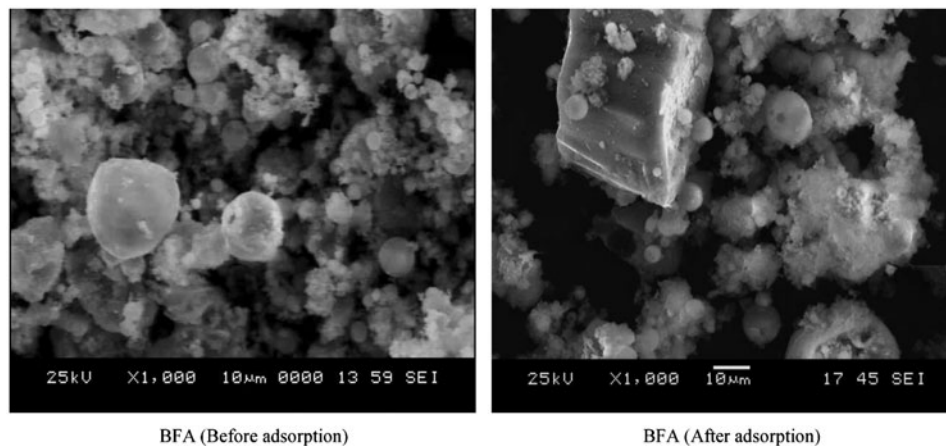


Fig. 1a. SEM image of BFA before and after adsorption.

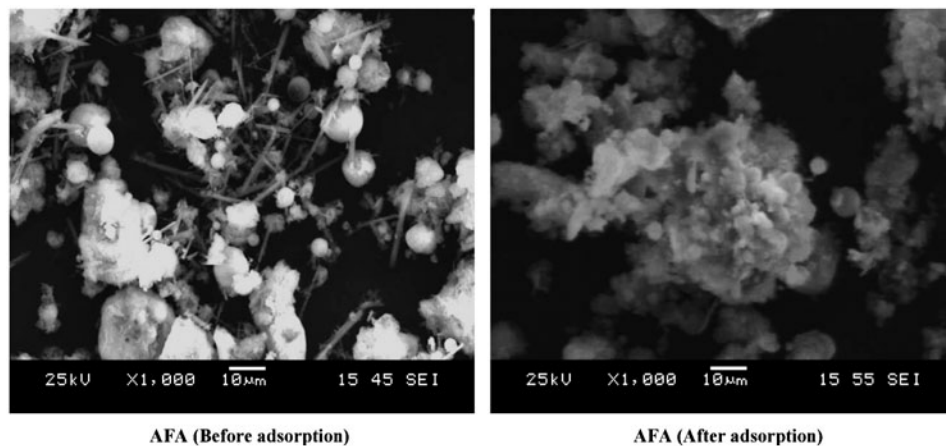


Fig. 1b. SEM image of AFA before and after adsorption.

Table 1
EDX analysis of BFA and AFA

Percentage of oxides present in BFA		Percentage of oxides present in AFA	
Compound	Mass	Compound	Mass
MgO	3.28	MgO	4.61
Al ₂ O ₃	36.36	Al ₂ O ₃	36.83
SiO ₂	38.10	SiO ₂	25.81
CaO	17.39	CaO	25.89
TiO ₂	2.55	TiO ₂	1.60
Fe ₂ O ₃	2.31	SO ₃	2.9
		Fe ₂ O ₃	2.36

2.1. Characterization of the adsorbents

2.1.1. Scanning electron microscopic studies (SEM)

Fly ash is a heterogeneous material consisting largely of small spheres formed by the condensation of aluminous and siliceous glass droplets in the air. Also found in fly ash samples are irregular, porous, coke-like particles of unburned carbon material, which are often concentrated in the larger size fractions. SEM is employed to observe the physical morphology of the Fly ash at 1,000 × g magnification.

SEM (Figs. 1a and 1b) image clearly shows that finer fly ash particles are primarily spherical, whereas

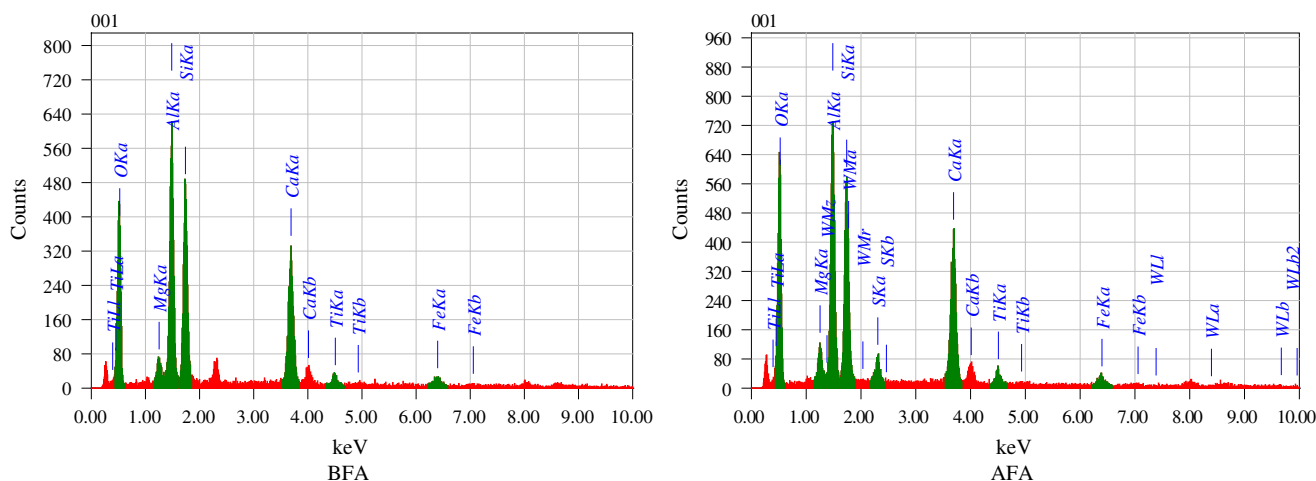


Fig. 2a. EDX spectrum for BFA and AFA before adsorption.

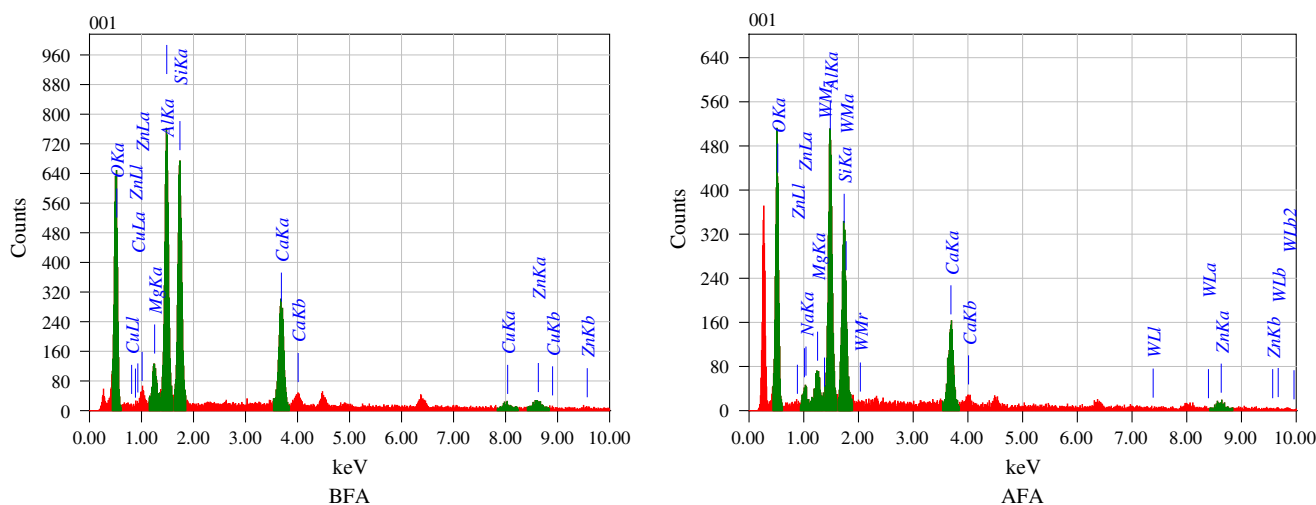


Fig. 2b. EDX spectrum for BFA and AFA after adsorption.

the coarser particles are mainly composed of irregular and porous particles in BFA and AFA, respectively.

The Figs. 1a and 1b shows the SEM image of BFA before and after adsorption of Zn(II) ions. The SEM and EDX analysis were done by using the instrument JEOL JED 2300 analysis station with different counting rates and different fitting coefficients.

2.1.2. EDAX Elemental Analysis

Table 1 shows the chemical composition of the BFA and AFA samples used in this study, respectively. SiO₂ and Al₂O₃ contents make up about 74% of the fly ash. FeO and CaO contents compose to about 19% (Fig. 2a). According to the ASTM C618, this fly ash can be classified as class F for having greater than 70% content of three components SiO₂, Al₂O₃, and Fe₂O₃. In Fig. 2b, the peaks at 1–2 and 8–10 in keV scale proves the adsorption of Zn(II) ions onto BFA and AFA.

2.1.3. Brunauer, Emmett and Teller's model of multi-layer adsorption (BET Isotherm)

In 1938, Stephen Brunauer, Paul Emmett, and Edward Teller developed a model isotherm that considers that possibility [8] (Figs. 3a and 3b).

Quantachrome Instruments, version 5.02, tested the low temperature adsorption of nitrogen (77.3 K) using BFA and AFA. The isotherms were shown in Figs. 3a and 3b. The specific surface area and total volume of pores of the adsorbents were determined using a simplified BET method described in the paper by Moellmer et al. [9]. The average pore radius, the pore volume, and the surface area of the BFA were 1.354e+2 Å, 3.113e–2 cc/g, and 4.598 m²/g, whereas the average pore radius, the pore volume, and the surface area of the AFA were 9.425e+01 Å, 2.032e–1 cc/g, and 43.111 m²/g, respectively. So Zn(II)

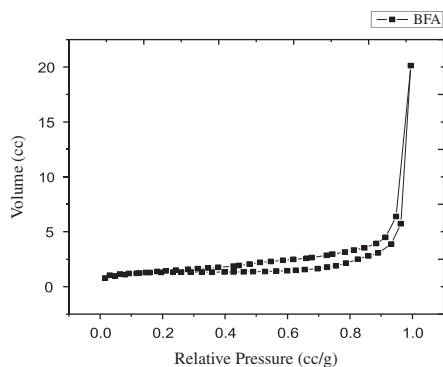


Fig. 3a. BET adsorption isotherm graph for BFA.

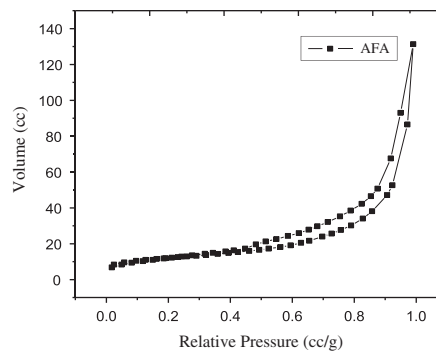


Fig. 3b. BET adsorption isotherm graph for AFA.

ions can be easily adsorbed onto the surface of the BFA and AFA. The surface area, average pore radius, and the pore volume of AFA was more compared to that of BFA.

2.2. Adsorption studies

A stock solution of ZnSO₄·7H₂O (1,000 mg L⁻¹) was prepared and suitably diluted accordingly to the various initial concentrations. Adsorption studies were carried out at room temperature (30 ± 1 °C). Batch adsorption studies were carried out using 0.2 g of Fly ash for each bottle, the adsorption experiments were carried out with 50 mL of solution of required concentration and pH of Zn(II) metal ion solutions varied from 2 to 10 in a bench shaker at a fixed shaking speed of 120 rpm. The resulting mixture was filtered (Whatmann filter paper No.41) and the initial and final concentration of the metal ions in the filtrate was determined via a UV-2450 vis spectrophotometer at the maximum adsorption wavelength (λ_{max}) of 213 nm [10]. The pH of the solution ranging 2–10 was brought by using 0.1 M HCl and 0.1 M NaOH. The pH of the solution was maintained in the desired pH by adding buffer solution (ethanoic acid and sodium ethanoate). The experiments were carried out for various adsorbent dosages, different initial Zn(II) ions concentration, various contact time, and pH. The Stock solution of ZnSO₄·7H₂O was prepared for the concentration of 1,000 ppm and it was further diluted to various required concentrations. From the initial and final concentration, the percentage removal can be calculated by

$$\% \text{ of Removal} = \frac{(C_0 - C_e) \times 100}{C_0} \quad (1)$$

where C₀ initial concentration of Zn(II) ions in mg L⁻¹, C_f final concentration of Zn(II) ions in mg L⁻¹.

Data obtained in batch mode kinetics were used to calculate the equilibrium metal uptake capacity. It was also calculated for adsorptive quantity of Zn(II) ions by using the following expression:

$$q_e = \frac{v \times (C_0 - C_e)}{w} \quad (2)$$

where q_e is the equilibrium metal ion uptake capacity in mg g^{-1} , v is the sample volume in L , C_0 the initial metal ion concentration in mg L^{-1} , C_e the equilibrium metal ion concentration in mg L^{-1} and w is the dry weight of adsorbent in grams.

3. Results and discussion

The adsorption experiments were carried out at different experimental conditions and the results obtained were discussed below.

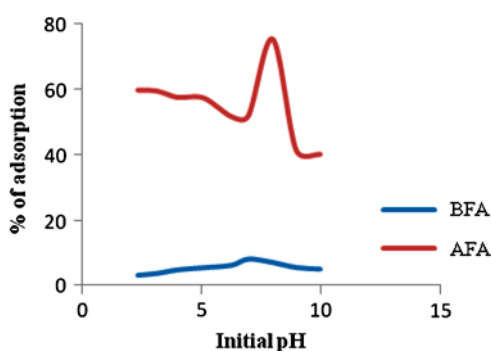


Fig. 4. The effect of solution pH on adsorption onto BFA and AFA.

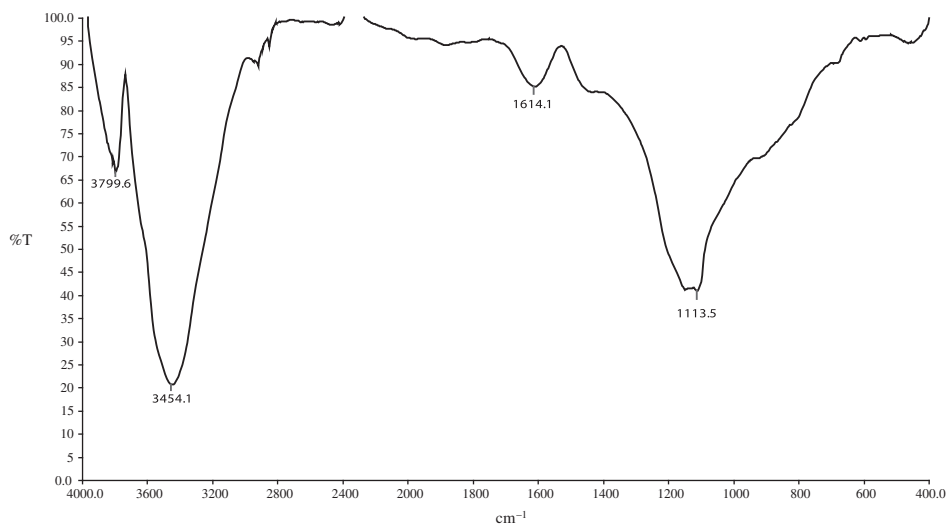


Fig. 5a. FTIR spectrum of BFA.

3.1. Batch mode study

3.1.1. Effect of pH (Fig. 4)

The effect of initial pH of the Zn(II) ion solution on the amount of adsorption was studied by varying the initial pH for both the adsorbent BFA and AFA under constant conditions of other parameters. The pH of BFA and AFA were 8.91 and 8.8, respectively. The pH_{ZPC} of the fly ash (BFA) was 3.06 and for AFA, the pH_{ZPC} was 2.13. The metal solution pH is above the pH_{ZPC} – the surface of the adsorbent was negatively charged and metal solution pH is below the pH_{ZPC} – the surface of the adsorbent was positively charged. Therefore, it was expected that positively-charged metal ions are likely to adsorb onto the negatively-charged fly ash particles at a pH above 3.06 for BFA and at a pH above 2.13 for AFA.

The change in pH value after adsorption of Zn(II) ions onto BFA and AFA was studied (Fig. 4) and an increase in pH value was noted. For BFA and AFA, the pH of the final solution slightly changed from pH 2 to 7. Greater increase in pH for the solution from 8 indicated the adsorption caused by the removal of Zn(II) ions due to the precipitation of Zn(II) ions as $\text{Zn}(\text{OH})_2$ in the alkaline solution pH rather than adsorption above the solution of pH 8 [11,12].

The surface acidity of BFA and AFA was the same (0.65 m mol/g) and the basicity was 3.62 m mol/g for BFA and 3.29 m mol/g for AFA.

Boehm titration shows the number of acidic, basic, phenolic, carboxyl, and lactones sites. For BFA, the number of basic sites present was 0.00896 mEq/g ; the phenolic, carboxyl, and lactone groups was 0.023 mEq/g ; and the carboxyl groups present was

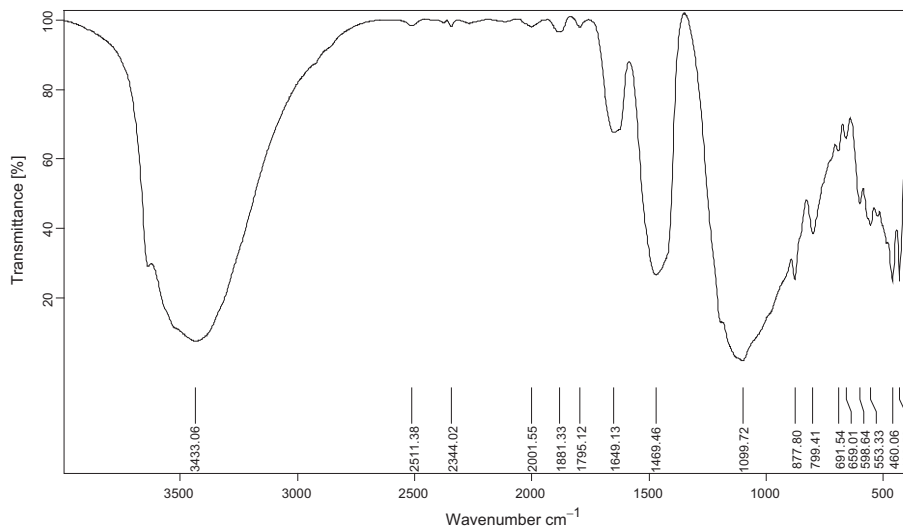


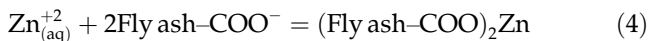
Fig. 5b. FTIR spectrum of AFA.

0.01138 mEq/g. For AFA, the number of basic sites present was 0.00762 mEq/g; the phenolic, carboxyl, and lactone groups was 0.0254 mEq/g; and the carboxyl groups present was 0.0138 mEq/g.

From the above results, the adsorption of Zn(II) ions onto BFA and AFA may be taking place at the carboxylic groups sites.

From FTIR analysis (Fig. 5a and Fig. 5b), the presence of broad band at 3454.1 cm^{-1} for BFA and at 3433.06 cm^{-1} for AFA indicates the presence of hydroxyl groups on the adsorbents. The presence of band at $1,600\text{--}1,800\text{ cm}^{-1}$ is corresponding to C=O group stretching of carboxylic acid from aldehydes and ketones [13]. The band appearing at 799.41 cm^{-1} corresponds to quartz present in AFA. The intensity of band at 462 cm^{-1} associated in all cases with Si–O bending vibrations of these adsorbents. The bands appearing between $800\text{ and }500\text{ cm}^{-1}$ are associated with the fragments of the aluminosilicate system. The presence of the functional groups, hydroxyl, carboxyl, phenyl, etc. is confirmed by Bohem titration as well.

Equilibrium reaction of metal adsorption considered as follows:



Due to high concentration of H^+ ions for the pH lower than 2, equilibrium of the reaction Eq. (3) will

be shifted to the left side according the equilibrium law. Since sites of ion exchange on the lignite-fired fly ash are mainly protonated, less available groups for ion exchange become available. As expected, the efficiency generally increases with increasing pH, while the effect of pH is inductive or even reverse. The increase of adsorption efficiency is the most explicit for pH values between 2 and 4, probably the reflecting progressive deprotonation of carboxyl groups ($-\text{COOH}$) from the lignite can lose H^+ and be appreciably deprotonated, which will shift the reaction Eq. (4) to the right, while the increase of the solution pH increases Zn(II) ions from the aqueous solution. Karthigayan et al. 2004 [14] observed hydrolysis reaction Eq. (5) at $\text{pH} \geq 6$ and Zn(II) ions hydroxide precipitation.

In the present study, optimum pH value was fixed as 7.0 for BFA and it was four for AFA where the maximum adsorption of metal ions occurs. The results are shown in Fig. 4. At pH 7, the percentage removal was about 8.3% for BFA and the maximum removal at pH 4 was 57.29% for AFA. The higher percentage of adsorption of Zn(II) ions may be due to the large pore volume and large surface area of AFA compared with BFA.

3.1.2. Effect of contact time

The effect of contact time on the amount of Zn(II) ions adsorption was observed at the optimum initial concentration of Zn(II) ion for BFA and for AFA. The extent of contact time on the amount of adsorption of Zn(II) ions by adsorbent was found to be increased

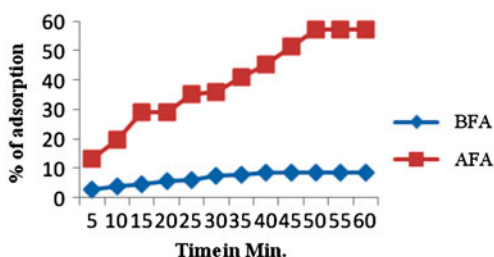


Fig. 6. Effect of time on adsorption of Zn²⁺ onto BFA and AFA.

and reached a maximum value with increase in contact time. Initially, the percentage of adsorption drastically increased and after 15 min, the percentage of adsorption increased steadily, and after 45 min, it attained equilibrium for AFA. This is because of the availability of adsorption site that may be higher initially and as the time increases, it decreases due to the occupation of adsorption sites. Initially for BFA, the percentage of adsorption drastically increased, after 15 min, the percentage of adsorption steadily increased, and after 40 min, it attained equilibrium. This is because of the higher availability of adsorption sites initially which decreases due to the occupation of adsorption sites as the time increases. The relative increase in the extent of removal of metal cation attained equilibrium after 40 min of contact time for BFA and after 45 min of contact time for AFA, which was fixed as the optimum contact time. The effect of contact time on adsorption is shown in Fig. 6.

3.1.3. Effect of initial concentration of metal cation

The effect of Zn(II) ion concentration on the extent of removal of Zn(II) ions (in terms of percentage removal) and amount adsorbed (q) were studied. The percentage removal was found to decrease with the increase in initial concentration of Zn(II) ion solution (Fig. 7) for both the cases. This indicates a decrease in adsorption which is attributed to the lack of active

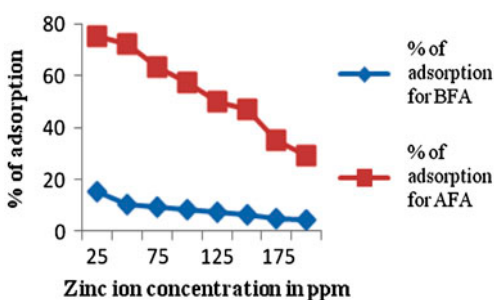


Fig. 7. Effect of Zn(II) ion concentration on adsorption.

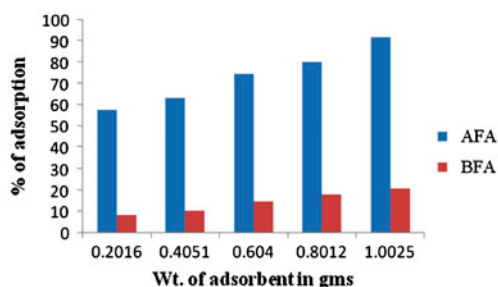


Fig. 8. Effect of dose variation on adsorption of Zn(II) ions.

sites, while increasing the initial concentration of Zn (II) ions. Similar results have been reported in literature on the extent of removal of metal ions [15].

3.1.4. Effect of dose of adsorbent

The effect of the dosage of adsorbent on adsorption of Zn(II) ion was studied for both BFA and AFA. The percentage removal increases with the increase in dose of both BFA and AFA adsorbents (Fig. 8). This may be due to the increase in availability of surface-active sites resulting from the increased dose and conglomeration of the adsorbent [16]. This suggests that the adsorbed species or solutes may either block the access to the internal pores or cause particles to aggregate thereby resulting in decrease in the availability of active sites for adsorption.

3.2. Kinetics

Fig. 6 shows the adsorption characteristics as a function of time. The kinetic experiments were performed by agitating the fly ash in bottles in a shaking bath for 1 h at 30°C. In these tests, 4 g of fly ash in 1 L of metals were used. The pH was 7.0 for BFA and 4.0 for AFA, where the precipitations for Zn(II) ions were relatively low. The metal ion concentrations were determined at varying intervals. As shown, the rate of uptake of metal removal in the first 40 min for BFA was 8.3% and in the first 45 min for AFA was 57.14% of the maximum removal of Zn(II) ions. Equilibrium was reached within 1 h for both fly ashes. However, only 8.3% of Zn(II) ions were removed from the solution at equilibrium indicating that more BFA was needed to remove Zn(II) ions compared with AFA.

The kinetics and dynamics of adsorption of Zn(II) ions metal ion adsorption have been studied by applying various kinetic equations.

Pseudo-first-order Lagergren equation:

$$\log q_e - \log q_t = \log q_o - \frac{t \times K_L}{2.303} \quad (6)$$

where K_L is the Lagergren constant and q_t is metal uptake at moment t .

Pseudo-second-order equation model developed by Ho and Mckay [17]

$$\frac{t}{qt} = \frac{1}{K_2 q_e^2} + \frac{t}{q_e} \quad (7)$$

where K_2 is the equilibrium rate constant for the pseudo-second-order adsorption ($\text{g mg}^{-1} \text{min}^{-1}$) and can be evaluated from the slope of the plot.

From the data obtained from kinetic experiments, the linear regression coefficient (R^2) for pseudo-first-order equation was 0.8774, whereas the R^2 value for pseudo-second-order equation was 0.963 for BFA (Table 2). The R^2 value for pseudo-second-order equation was close to unity compared with pseudo-first-order R^2 value (0.88). So it was confirmed that the adsorption of Zn(II) ions on BFA follows pseudo-second-order kinetics. The adsorption maximum value was 2.844 for first-order and for second-order kinetics, $q_e = 1.06$, which was nearer to the experimental q_e value (1.66). Similarly, for AFA, the R^2 value for pseudo-first-order equation was 0.64, whereas the R^2 value for pseudo-second-order equation was 0.905 for AFA. The R^2 value for pseudo-second-order equation was close to unity compared with pseudo-first-order R^2 value (0.64). So it was confirmed that the adsorption of Zn(II) ions on AFA also follows pseudo-second-order kinetics. The adsorption capacity for both the adsorbents were compared and found to be higher for AFA ($q_e = 22.7$) than for BFA ($q_e = 1.06$). The adsorption maximum value (q_e) was 23.7 for first-order kinetics and the q_e value was 22.7 for second-order kinetics for AFA. The experimental q_e value was 9.6, which was compared and found nearer to the q_e obtained from second-order kinetics (22.7) than from first-order kinetics (23.7). This also confirms the fitness of pseudo-second-order kinetics for both the adsorbents. This suggests that this sorption system is not a first-order reaction and that the pseudo-second-order model based on the assumption that the rate limiting step may be chemical sorption or chemisorptions involving valence forces through sharing or exchange of electrons between sorbent and sorbate provides the best correlation of the data. The initial sorption rate " h " can be regarded as $q_t/t \rightarrow 0$, hence: $h = kq_e^2$. The h value for BFA was only 0.013 and for AFA, it was 38.23 which proves the higher adsorption of Zn(II) ions onto AFA than BFA. If pseudo-second-order kinetics are applicable, the plot of t/qt against t of second-order equation should give a linear relationship from which q_e , k , and h can be determined from the slope and intercept of the plot. The adsorption process of pollutants from

more component systems can be fitted well using the pseudo-second-order rate for both BFA and AFA.

In addition, the same data were plotted with the Elovich Eq. (8). From the equation, the correlation coefficient (R^2) was 0.942 for BFA and was 0.923 for AFA. The Elovich equation is another rate equation based on adsorption capacity generally expressed as [18–20]:

$$\frac{dq_t}{dt} = BE \exp(-A_E q_t) \quad (8)$$

where q_t is the sorption capacity at time t (mg g^{-1}), A_E is the initial sorption rate ($\text{mg g}^{-1} \text{min}^{-1}$) and B_E is the desorption constant (g mg^{-1}) during any one experiment. The initial adsorption rate A_E for BFA (1.54) and for AFA (0.2161) and the desorption constant B_E was higher for AFA (75.25) than BFA (3.64). The above result also proves the higher adsorption capacity of AFA for Zn(II) ions. Thus, the constants can be obtained from the slope and the intercept of a straight line plot of qt against $\ln(t)$. Eq. (8), used to test the applicability of the Elovich equation to the kinetics of sorption.

The possibility of intraparticle model diffusion was explored by using the Weber and Morris intraparticle diffusion model [21].

$$qt = K_p t^{1/2} + C \quad (9)$$

where q_t – amount of Zn(II) ion adsorbed at time, t (mg g^{-1}), C – intercept, K_d – intraparticle diffusion rate constant ($\text{mg g}^{-1} \text{min}^{-1/2}$).

The values of q_t were linearly correlated with values of $t^{1/2}$. The K_d values were calculated by using correlation analysis. $K_d = 0.282$, $C = 0.123$, $R^2 = 0.929$ for BFA and $K_d = 2.052$, $C = 1.63$, $R^2 = 0.963$ for AFA. From the value of C , the thickness of the adsorption layer was found to be higher for AFA than BFA.

According to Ho et al. [22], if the intraparticle diffusion is the sole rate-limiting step, it is essential for the q_t vs $t^{1/2}$ plots to pass through the origin, which is observed in Fig. 9; it may be concluded that

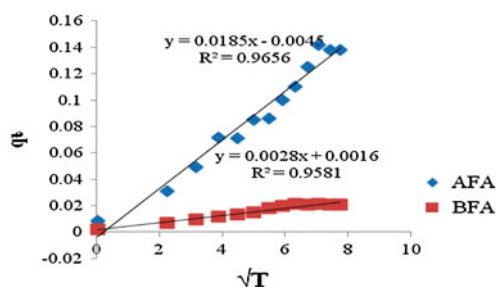


Fig. 9. Intraparticle diffusion of BFA and AFA.

Table 2
Kinetic parameters for the adsorbents BFA and AFA for Zn(II) ion

	Pseudo-first order equation		Pseudo-second order equation		Elovich equation		Intraparticle diffusion							
	K_1 (s^{-1})	q_e cal. (mg/g)	R^2	K_2 (L mole $^{-1}$ S $^{-1}$)	q_e cal. (mg/g)	H	R^2	A_E (mg/g min)	B_E (g/min)	R^2	K_d (mg/g min $^{1/2}$)	R	C	
BFA	1.66	0.083	2.844	0.88	0.012	1.058	0.013	0.963	1.524	3.6385	0.942	0.284	0.928	0.123
AFA	9.6	0.0691	23.66	0.64	0.074	22.7	38.23	0.905	0.216	75.25	0.923	2.052	0.963	1.63

the surface adsorption and intraparticle diffusion were concurrently operating during the metal ion and adsorbent (BFA and AFA) interactions [23].

3.3. Isotherm data analysis

In order to optimize the design of an adsorption system to remove the heavy metal, it is important to establish the most appropriate correlations of the equilibrium data of each system. The parameters obtained from the different models provide important information on the adsorption mechanisms, the surface properties, and affinities of the adsorbent. The correlation with the amount of adsorption and the liquid-phase concentration was tested with the Langmuir, Freundlich, Tempkin, and Dubinin–Rudushkevich (D–R) isotherm equations. Linear regression is used often to determine the best-fitting isotherm, and the applicability of isotherm equations is compared by judging the correlation coefficients [23].

The equilibrium data for the metal ion over the concentration range from 5 to 200 mg/L at $30 \pm 1^\circ\text{C}$, which have been correlated with the Langmuir isotherm [24].

$$q_e = \frac{Q_m K_a C_e}{(1 + K_a C_e)} \quad (10)$$

In Eq. (6), C_e and q_e are defined before in Eq. (2), Q_m is a constant and reflects a complete monolayer (mg g^{-1}); K_a is adsorption equilibrium constant (L mg^{-1}) that is related to the apparent energy of sorption. A linear plot is obtained when C_e/q_e is plotted against C_e over the entire concentration of the metal ion investigated.

The results obtained from the Langmuir model for the removal of Zn(II) ions on BFA and AFA are shown in Table 3.

The correlation coefficients reported in Table 3 showed strong positive evidence for the adsorption of Zn(II) metal ion onto BFA and AFA which fitted well the Langmuir isotherm model. The applicability of the linear form of Langmuir model to BFA and AFA was proved by the high correlation coefficients R^2 compared with other isotherms. This suggests that the Langmuir isotherm provides a good model of the sorption system. The maximum monolayer capacity of Q_m obtained from the Langmuir is 1.03 mg g^{-1} for BFA and 5.695 mg g^{-1} for AFA. These results show that for heavy metals, adsorption capacity was high for AFA compared with BFA.

The Freundlich sorption isotherm, one of the most widely used mathematical description of adsorption,

usually fits the experimental data over a wide range of concentrations. This isotherm gives an expression encompassing the surface heterogeneity and the exponential distribution of active sites and their energies. The Freundlich isotherm was also applied for the removal of Zn (II) ions from BFA and AFA.

$$qe = K_F C_e^{1/n} \quad (11)$$

where K_F is a constant for the system related to the bonding energy. The adsorption or distribution coefficient K_F represents the quantity of metal ions adsorbed onto adsorbent for unit equilibrium concentration. $1/n$ is indicating the adsorption intensity of metal ion onto the adsorbent or surface heterogeneity becoming more heterogeneous as its value gets closer to zero. A value for $1/n$ not equal to zero indicates a normal Langmuir isotherm, while above 1 is indicative of cooperative adsorption.

The applicability of the Freundlich adsorption isotherm was also analyzed using the same set of experimental data by plotting $\log(q_e)$ versus $\log(C_e)$ [25–27]. The data obtained from linear Freundlich isotherm plot for the adsorption of the Zn(II) ions ion onto BFA and AFA is presented in Table 3.

The correlation coefficient $R^2=0.95$ for BFA and $R^2=0.9343$ for AFA from Langmuir model were close to unity compared with other studied isotherm models that showed the applicability of the Langmuir model for both the adsorbents. It proved the monolayer homogeneous adsorption behaviour of both the adsorbents. The $1/n$ value was not equal to 0 showed that the adsorption of Zn(II) ions onto both adsorbents was not a heterogeneous adsorption.

The Tempkin adsorption isotherm model has been applied commonly in the following form [28–30]:

$$qe = \frac{RT}{b} \ln(AC_e) \quad (12)$$

where $\beta = (RT)/b$, T is the absolute temperature in Kelvin and R is the universal gas constant, $8.314\text{ J (molK)}^{-1}$. The constant related to the heat of adsorption [28]. The examination of the data shows that the Tempkin isotherm fitted well for the adsorption of the Zn(II) ions on to BFA than AFA from the correlation coefficient shown in the Table 3.

The D-R model was applied to estimate the porosity, apparent free energy, and the characteristics of adsorption [31–33]. The D-R isotherm does not assume a homogeneous surface or constant adsorption potential. The D-R model has commonly been applied in the following Eq. (13).

$$qe = Q_m \exp(-K\varepsilon^2) \quad (13)$$

where K is a constant related to the adsorption energy, Q_m the theoretical saturation capacity, ε the Polanyi potential, calculated from Eq. (14).

$$\varepsilon = RT \ln\left(1 + \frac{1}{C_e}\right) \quad (14)$$

The slope of the plot of $\ln q_e$ versus ε^2 gives K ($\text{mol}^2 (\text{kJ}^2)^{-1}$) and the intercept yields the adsorption capacity, Q_m (mgg^{-1}). The mean free energy of adsorption (E), defined as the free energy changes when one mole of ion is transferred from infinity in solution to the surface of the solid, was calculated from the K value using the following relation [34,35].

$$E = \frac{1}{\sqrt{2K}} \quad (15)$$

The calculated value of D–R parameters is given in Table 3. The saturation adsorption capacity Q_m obtained using D–R isotherm model for adsorption of Zn(II) ions onto BFA and AFA is 23.51 mgg^{-1} and 8.587 mgg^{-1} at $0.2 \text{ g}/50 \text{ mL}^{-1}$ adsorbent dose, respectively. The values of E calculated using Eq. (15) is

Table 3
Isotherm constants and coefficients of determinations for BFA and AFA

Isotherm model	BFA	AFA	Isotherm model	BFA	AFA
Langmuir			Tempkin		
Q_m (mg g^{-1})	1.03	5.695	α (L g^{-1})	2.91	4.904
K_a (L mg^{-1})	0.031	0.0458	β (mg L^{-1})	1.1695	0.8629
R^2	0.950	0.9343	b	2154.03	2919.4
Freundlich			R^2	0.9823	0.9162
$1/n$	0.5379	0.8962	Dubinin–Radushkevich		
K_F (mg g^{-1})	20.78	363.245	Q_m mg g^{-1}	23.51	8.587
R^2	0.9534	0.9002	K ($\times 10^{-5} \text{ mol}^2 \text{ kJ}^{-2}$)	0.163	9
	R^2	0.9634	E (kJ mol^{-1})	0.00175	0.075
			0.7267		

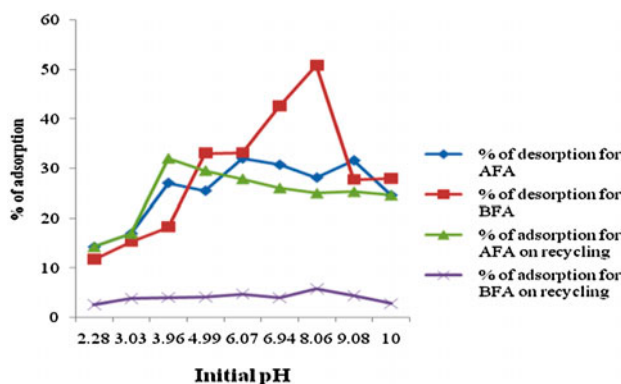


Fig. 10. Percentage of desorption and adsorption on recycling of BFA and AFA.

0.00175 for BFA and 0.075 for AFA, which indicates that the physico-sorption process also plays a significant role in the adsorption of Zn(II) ions (II) ions onto AFA compared to BFA.

3.4. Desorption and recycling studies

Desorption studies were carried out for both the adsorbent BFA and AFA by employing batch methods [7]. Equal amount of Zn(II) ions-loaded adsorbents were taken in nine bottles and 50 mL of extraction water whose pH was adjusted from 2 to 10 using 0.1 N HCl/NaOH was added. These bottles were kept on a bench shaker for 1.30 h. The metal ion concentration of solution was measured using UV-2450 spectrophotometer at the wavelength λ_{\max} 213 nm. However, 50.9% of adsorbed Zn(II) ions was desorbed at pH 8 as in the case of BFA and from AFA, the amount of Zn(II) ions desorbed was found to be 33.19% at pH 6.

The adsorbent, which was desorbed by the above said method, was used for adsorption again. The adsorption ability for both BFA and AFA was studied by batch modes. On recycling, the maximum adsorption percentage was reached at the pH 7 and it was found to be 6% for BFA and 32% at pH 4 AFA. These results show that the adsorbent AFA can be reused for adsorption compared with BFA and the recycling capacity for both the adsorbents was shown in Fig. 10. Desorption and recycling for the adsorbents were done thrice.

4. Conclusion

The adsorption of Zn(II) ions is pH dependent with maximum adsorption occurring at pH 4 for AFA compared with BFA. The adsorption data fitted well

by the Langmuir isotherm model compared with Freundlich, Tempkin and D-R isotherm models. The kinetic studies of Zn(II) on BFA and AFA were performed based on pseudo-first-order, pseudo-second-order, Elovich, and intraparticle diffusion equations. The data indicate that the adsorption of Zn(II) ions onto BFA and AFA followed the pseudo-second-order rate with intraparticle diffusion as one of the rate determining steps. The present study concludes that the adsorption of Zn(II) ions onto Lignite-fired AFA was found to be approximately five times higher than for the fly ash taken without washing. The desorption studies indicate that the Zn(II) ions adsorbed onto BFA and AFA are moderate and 50% of the ions could be recovered in a batch process from both the adsorbents using distilled water at pH 8 for BFA and at pH 6 for AFA. The recycling process also indicates that the adsorbent may be reused for adsorption process. Thus, the lignite-fired AFA can be used for the removal of Zn(II) ions from aqueous solution.

References

- [1] I. Ayhan Sengila, M. Ozacar, Competitive biosorption of Pb^{2+} , Cu^{2+} and Zn^{2+} ions from aqueous solutions onto tannin resin, *J. Hazard. Mater.* 166 (2009) 1488–1494.
- [2] O.A. Ali, S.J. Tarek, Removal of polycyclic aromatic hydrocarbons from Ismailia canal water by chlorine, chlorine dioxide and ozone, *Desalin. Water Treat.* 1 (2009) 289–298.
- [3] A.K. Chakravarthy, S. Chowdhury, S. Chakravarthy, Q.C. Mukherjee, Liquid membrane multiple emulsion ion process of chromium (VI) separation from wastewater, *Colloids Surf A: Physicochem. Eng. Aspects* 103 (1995) 59–71.
- [4] J.H. Choi, S.D. Kim, Y.J. Kwon, W.J. Kim, Adsorption behaviours of ETS-10 and its variant, ETAS-10 on the removal of heavy metals, Cu^{2+} , Co^{2+} , Mn^{2+} , and Zn^{2+} , from a waste water, *J. Microporous Mesoporous Mater.* 96 (2006) 157–167.
- [5] A.G.M. Silva, M.O. Hornes, M.L. Mitterer, M.I. Queiroz, Application of coagulants in pre-treatment of fish wastewater using factorial design, *Desalin. Water Treat.* 1 (2009) 208–214.
- [6] L. Wei, K. Wang, Q. Zhao, C. Xie, W. Qiu, T. Jia, Kinetics equilibrium of adsorption of dissolved organic matter fraction from secondary effluent by FA, *J. Environ. Stud.* 23 (2011) 1057–1065.
- [7] R.A. Khan RaO, M.A. Khan, F. Rehman, Batch and column studies for the removal of lead(II) ions from aqueous solution onto lignite, *Ad. Sci.Tech.* 29 (2011) 83–98.
- [8] S. Brunauer, P.H. Emmett, E. Teller, Adsorption of gases in multi molecular layers, *J. Am. Chem. Soc.* 60 (1938) 309–315.
- [9] J. Moellmer, E.B. Celer, R. Luebke, A.J. Cairns, R. Staudt, M. Eddaoudi, M. Thommes, Insights on adsorption characterization of metal-organic frameworks: A Benchmark study on the novel SOC-MOF, *Microporous Mesoporous Mater.* 129 (2010) 345–353.
- [10] L. Wei, K. Wang, Q. Zhao, C. Xie, W. Qiu, T. Jia, Kinetics and equilibrium of adsorption of dissolved organic matter fractions from secondary effluent by fly ash, *J. Environ. Sci.* 23(7) (2011) 1057–1065.
- [11] H. Cho, D. Oh, K. Kim, A study on removal characteristics of heavy metals from aqueous solution by fly ash, *J. Hazard. Mater.* 9 (2005) 187–195.

- [12] B. Zhu, T. Fan, D. Zhang, Adsorption of copper ions from aqueous solution by citric acid modified soybean straw, *J. Hazard. Mater.* 153 (2008) 300–308.
- [13] A. Saeed, M. Iqbal, M.W. Akhtar, Removal and recovery of lead(II) from single and multi metal (Cd, Cu, Ni, Zn) solutions by crop milling waste (black gram husk), *J. Hazard. Mater.* 117 (2005) 65–73.
- [14] G. Karthikeyan, K. Anbalagan, N. Muthulakshmi Andal, Adsorption dynamics and equilibrium studies of Zn (II) onto chitosan, *J. Chem. Sci.* 116 (2004) 119–127.
- [15] B. Bayat, Comparative study of adsorption properties of Turkish fly ashes I. The case of nickel(II), copper(II) and Zn (II) ions, *J. Hazard. Mater.* 95 (2002) 251–273.
- [16] N. Kannan, K. Karuppasamy, Low cost adsorbents for the removal of phenyl acetic acid from aqueous solution, *Indian J. Environ. Prot.* 18 (1998) 683–690.
- [17] Y.S. Ho, McKay Pseudo – second order model for sorption processes, *Process Biochem.* 34 (1999) 51–465.
- [18] S.H. Chin, W.R. Clayton, Application of Elovich equation to the kinetics of phosphate release and sorption on soil, *Soil Sci. Soc. Am. J.* 44 (1980) 265–268.
- [19] D.L. Sparks, Kinetics of Reaction in Pure and Mixed Systems, in: *Soil Physical Chemistry*, CRC Press, Boca Ration, FL, 1986.
- [20] J. Zeldowitsch, Über den mechanismus der katalytischen oxidation von CO an MnO_2 , *Acta Physicochim. URSS* 1 (1934) 364–449.
- [21] W.J. Weber Jr., J.C. Morris, Kinetics of adsorption on carbon from solution, *J. Sanit. Eng. Div. ASCE.* 8 (1963) 31–59.
- [22] Y.S. Ho, Removal of copper ions from aqueous solution by tree fern, *Water Res.* 37 (2003) 2323–2330.
- [23] T. Santhi, S. Manonmani, T. Smitha, Removal of malachite green from aqueous solution by activated carbon prepared from the epicarp of *Ricinus communis* by adsorption, *Desalin. Water Treat.* 20 (2010) 160–167.
- [24] I. Langmuir, The constitution and fundamental properties of solids and liquids, *J. Am. Chem. Soc.* 38 (1916) 2221–2295.
- [25] H.M.F. Freunlich, Über die adsorption in lösungen [Over the adsorption in solution], *Z. Phys. Chem.* 57 (1906) 385–470, (Leipzig).
- [26] D. Zhang, H. Hea, W. Lia, T. Gaoa, P. Maa, Biosorption of cadmium(II) and lead(II) from aqueous solutions by fruiting body waste of fungus *flammulina velutipes*, *Desalin. Water Treat.* 20 (2010) 160–167.
- [27] Y. Chen, D. Zhang, M. Chen, Y. Ding, Biosorption properties of cadmium(II) and Zn(II) ions from aqueous solution by tea fungus, *Desalin. Water Treat.* 8 (2009) 118–123.
- [28] C. Aharoni, M. Ungarish, Kinetics of activated chemisorption. Part 2. Theoretical models, *J. Chem. Soc. Faraday Trans.* 73 (1977) 456–464.
- [29] X.S. Wang, Y. Qin, Equilibrium sorption isotherms for Cu^{2+} on rice bran, *Process Biochem.* 40 (2005) 677–680.
- [30] G. Akkaya, A. Ozer, Adsorption of acid red 274 (AR 274) on *dicranella varia*: Determination of equilibrium and kinetic model parameters, *Process Biochem.* 40 (2005) 3559–3568.
- [31] C.J. Pearce, J.R. Lloyd, J.T. Guthrie, The removal of colour from textile wastewater using whole bacterial cells: A review, *Dyes Pigm.* 58 (2003) 179–196.
- [32] M.M. Dubinin, The potential theory of adsorption of gases and vapors for adsorbents with energetically non-uniform surface, *Chem. Rev.* 60 (1960) 235–266.
- [33] M.M. Dubinin, Modern state of the theory of volume filling of micropore adsorbents during adsorption of gases and steams on carbon adsorbents, *Zh. Fiz. Khim.* 39 (1965) 1305–1317.
- [34] L.V. Radushkevich, Potential theory of sorption and structure of carbons, *Zh. Fiz. Khim.* 23 (1949) 1410–1420.
- [35] M. Matheswaran, Kinetic studies and equilibrium isotherm analyses for the adsorption of methyl orange by coal fly ash from aqueous solution, *Desalin. Water Treat.* 29 (2011) 241–251.